Understanding the EOT-J_g degradation in Ru/$SrTiO_x$/Ru metal-insulator-metal capacitors formed with Ru atomic layer deposition

M. Popovici[1], A. Redolfi[1], M. Aoulaiche[2], J. A. van den Berg[3], B. Douhard[1], J. Swerts[1], P. Bailey[3], B. Kaczer[1], B. Groven[1], J. Meersschaut[1], T. Conard[1], A. Moussa[1], C. Adelmann[1], A. Delabie[1,4], P. Fazan[2], S. Van Elshocht[1], M. Jurczak[1]

[1] imec, Kapeldreef 75, B-3001 Leuven, Belgium
[2] Micron Technology resident at imec, Kapeldreef 75, 3001 Leuven, Belgium
[3] University of Huddersfield, International Institute for Accelerator Applications, Huddersfield, HD1 3DH, UK
[4] KU Leuven (University of Leuven), Department of Chemistry, Celestijnenlaan 200F, 3001 Leuven, Belgium

Abstract

The impact of different Ru precursors and/or deposition methods on the electrical characteristics of Ru/$SrTiO_x$/Ru capacitors has been investigated. The observed increase of the leakage current density (J_g) and the equivalent oxide thickness (EOT) for ALD (atomic layer deposition) deposited Ru layers compared to PVD (Physical vapor deposition) deposited ones was found to be caused by a $SrRuTiO_x$ layer formation at the $SrTiO_x$/Ru interface aided by the presence of the oxygen co-reactant used during the ALD, regardless of the precursor used.

Keywords: Metal-Insulator-Metal Capacitor; Strontium titanate; Ruthenium; Atomic Layer Deposition.

1. Introduction*

The continuous downscaling of the dynamic random access memory (DRAM) technology requires metal-insulator-metal capacitors (MIMCAP) deposited by conformal techniques such as atomic layer deposition (ALD) or chemical vapor deposition (CVD). We have demonstrated the potential of MIMCAPs based on a 5 nm Ru/8.5 nm $SrTiO_x$ (STO)/5 nm Ru layer structure to reach a leakage current density of 10^{-7} A/cm^2 at both +1V and −1V and room temperature for an 0.4 nm EOT. In this case, the Ru bottom electrode was grown by plasma enhanced atomic layer deposition and the Ru top electrode (TE) by physical vapor deposition (PVD) [1, 2]. However, with none of the conformal Ru processes, the low leakage levels achieved with a PVD Ru TE could be reproduced [2]. In order to understand what causes the increase of both the EOT and J_g, the impact of different ALD grown Ru top electrodes on the electrical characteristics of Ru/$SrTiO_x$/Ru based capacitors was investigated and compared with that of a Ru PVD TE. The information acquired from the electrical measurements in conjunction with high resolution depth profiling data showed that intermixing occurs at the STO/Ru TE interface to which the degradation of both the EOT and J_g is ascribed.

2. Experimental

The complete MIMCAP structure consists of a TiN/Ru/STO/Ru/TiN stack. The STO films were deposited on top of 5 nm Ru PEALD, grown on 10 nm PVD TiN, The top electrode was made of 5 nm Ru (grown by ALD or PVD) followed by 35 nm PVD TiN. For ALD, a zero-valent and a bivalent Ru precursor were used, namely (ethylbenzyl) (1-ethyl-1,4-cyclohexadienyl) Ru(0) (denoted EBECHRu) and cis-dicarbonyl bis(5-methylhexane-2,4-dionate) ruthenium(II) (denoted Carish). In both cases, O_2 was required as co-reactant for the deposition of metallic Ru. The Ru films were deposited on Sr-rich $SrTiO_x$ (~54% and 57% Sr) in a cross-flow, hot wall reactor at temperatures ranging between 225ºC and 325ºC [3]. The growth of the Ru films in terms of the amount of Ru deposited (atoms/cm^2) was monitored by Rutherford backscattering spectrometry (RBS) measurements. Elastic recoil detection (ERD), secondary ion mass spectrometry (SIMS) and angle-resolved X-ray photoelectron spectra (ARXPS) were used to determine elemental film composition and chemical depth profiles, respectively. Information about thin film interfacial reactions, layer thickness and structure was provided by Medium Energy Ion Scattering (MEIS) spectroscopy. The roughness of the Ru films was determined with atomic force microscopy (AFM). Planar MIM capacitors with a size of (100 × 100) µm^2 were fabricated on 300 mm diameter wafers using a one mask process in which only the Ru/TiN TE was patterned. EOT values were extracted at 0V from C-V curves measured at 10kHz, while J_g was measured at +/− 1V using a delay time of 0.1s [4].

3. Results and discussion

Metallic Ru films were deposited on STO substrates from EBECHRu and Carish precursors using an O_2 co-reactant. The

* Corresponding author Tel.: *+32 16 28 7759* popovici@imec.be

ALD reaction cycle consist of the sequence: O_2 pulse/O_2 purge/Ru precursor pulse/Ru precursor purge. The O_2 pulse was limited to 0.4 s and 0.1 s durations for the 5 s EBECHRu and the 3 s Carish depositions, respectively. At a deposition temperature of 225 ºC, no growth of Ru from the Carish/O_2 process was observed while the EBECHRu/O_2 one led to metallic Ru after a long incubation process of ~70 cycles. Increasing the deposition temperature to 275 ºC resulted in the growth of metallic Ru from both precursors with a further reduction in the number of cycles for incubation. At 325 ºC, incubation occurred up to ~10 cycles for the Ru Carish precursor while for the EBECHRu one still ~55 cycles were needed (Figure 1).

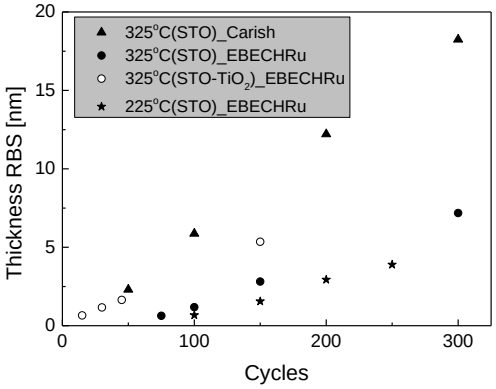

Fig. 1. Growth rates of Ru as a function of substrate type and Ru precursor as extracted from the number of cycles vs. Ru coverage measured by RBS and converted in thickness at a deposition temperature at 325ºC.

Less incubation i.e. faster layer closure, will result in a more 2D-like growth behavior and consequently a smoother film [5]. Therefore, we observed a lower roughness of ~0.4 nm rms for the 5 nm thick Ru films derived from the Carish precursor as compared to ~0.6 nm rms in the case of EBECHRu precursor, in both cases as grown at 325 ºC. On the other hand, the EBECHRu derived Ru films have a higher purity (C and H below 1% and O ~ 2%), while for the Carish derived Ru these are about two times higher. This is due to the fact that at a deposition temperature of 325 ºC the Carish precursor starts to decompose and a CVD component is present in the films. This could also explain the higher growth rate of 0.063 nm/cycle in the Carish process as compared to 0.030 nm/cycle for EBECHRu one. An increase of the film growth per cycle (GPC) for Ru films derived from the EBECHRu precursor to 0.035 nm/cycle was observed after the deposition of a thin cap layer of TiO_2 on STO. In this case, nucleation of Ru was enhanced and in fact no incubation was observed. Electrical characteristics (EOT-J_g) were determined for MIMCAPs with a Ru TE deposited via ALD and compared with a reference sample having a PVD grown Ru layer as the TE [1, 2]. When EBECHRu was used as the precursor, an increase of EOT of +0.19 nm was observed together with an increase of about two orders of magnitude in J_g at +1V, as compared with the reference sample having a PVD grown Ru layer as TE (Figure 2a). When a 1 nm thick TiO_2 interlayer was deposited on STO prior to Ru ALD, the EOT increase was limited to only +0.09 nm concomitant with an increase in J_g at +1V of about one order of magnitude. This suggests that a certain protective role is played by the TiO_2. This hypothesis is supported by the EOT-J_g values obtained for a thinner TiO_2 cap layer (0.5 nm), where the measured J_g at +1V was increased further. However, in all cases, J_g at −1V registered an even higher level (Figure 2b). This due to the fact that ALD TiO_2 (deposited using $Ti(OCH_3)_4$ and H_2O as precursors) results in anatase phase, which imply a low dielectric constant (maximum 40) and rather leaky layer [6]. Therefore the use of TiO_2 capping layer in the stack could not finally meet the EOT and leakage current requirements [7].

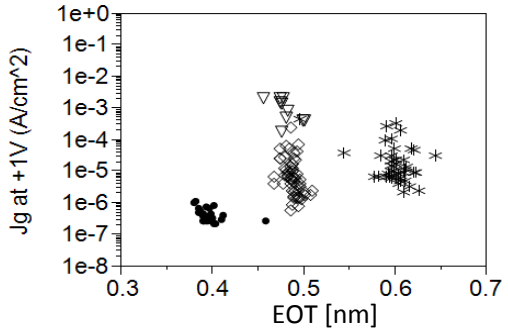

Fig.2a. EOT-J_g at +1V : Ru PVD (•), Ru EBECHRu (∗), Ru EBECHRu with a 0.5 nm TiO_2 (▽), Ru EBECHRu with a 1 nm TiO_2 interlayer (◇).

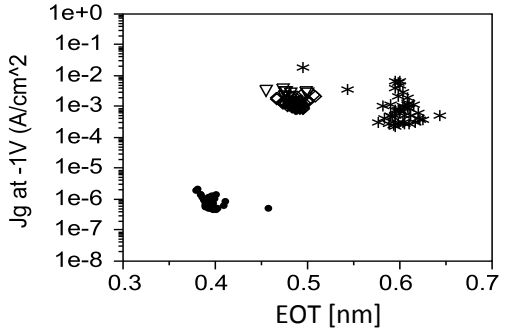

Fig.2b. EOT-J_g at -1V: Ru PVD (•), Ru EBECHRu (∗), Ru EBECHRu with a 0.5 nm TiO_2 (▽), Ru EBECHRu with a 1 nm TiO_2 interlayer (◇).

Double sweep current leakage density - applied voltage (J_g-V_g) curves (Figure 3) showed that ALD of the Ru top electrode results in a substantial increase of the leakage current, particularly at negative bias as compared to PVD Ru TE.

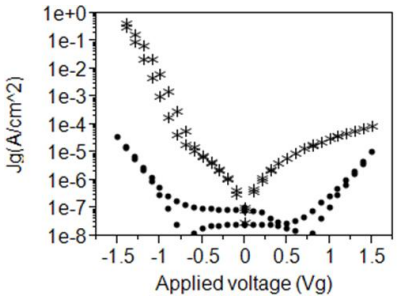

Fig.3. Double sweep J_g-V_g of Ru PVD (•) and Ru EBECHRu (∗).

This is interpreted as a trap-assisted current due to defect generation at the top electrode caused by SrO out-diffusion from the STO dielectric into Ru, to be discussed further in this section. Note that a spatially asymmetric defect distribution will generally influence the entire J_g-V_g characteristic, explaining the leakage increase at positive V_g. Aspects also

investigated are the effect of the Sr content and the thickness of the STO films on the EOT-J_g behavior. Until now electrical measurements were performed on MIMCAPs with a 8.5 nm thick STO layer having a 54% Sr content. Upon raising the Sr content to about 57% and reducing the physical thickness to ~ 7.2 nm, the J_g was increased further to ~ 10^{-1} A/cm^2 and the EOT by +0.22 nm for a Ru TE derived from a EBECHRu precursor as compared to Ru grown by PVD (~10^{-6} A/cm^2). In the case of the Carish derived Ru TE, an EOT increase of +0.11 nm was observed simultaneously with an increase in J_g of two orders of magnitude. This behavior was similar to that of the EBECHRu derived TE after a H_2 post-anneal at 325 ºC for 5 min (Figure 4a). In fact the H_2 post-treatment did also slightly reduce the J_g at −1V (Figure 4b). These results lead to the preliminary conclusion that two factors influence the EOT-J_g degradation. The first is the O_2 impact during Ru deposition at the temperature of 325 ºC which is related to the pulse length and incubation time. Increasing these parameters resulted in an EOT increase of up to ~ 0.2 nm with an increase in J_g. The second is the Sr content in the STO film.

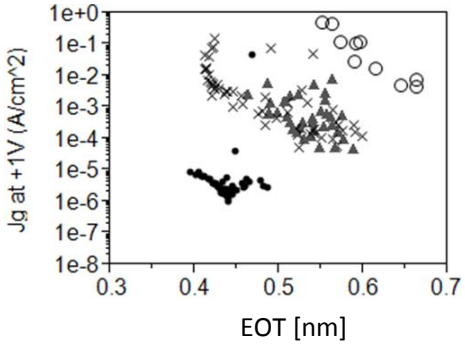

Fig.4a. EOT-J_g values at +1V: Ru PVD (•), Ru EBECHRu at 325ºC (o), Ru Carish at 325ºC (▲), Ru EBECHRu with 5 min H_2 post-anneal at 325ºC (x).

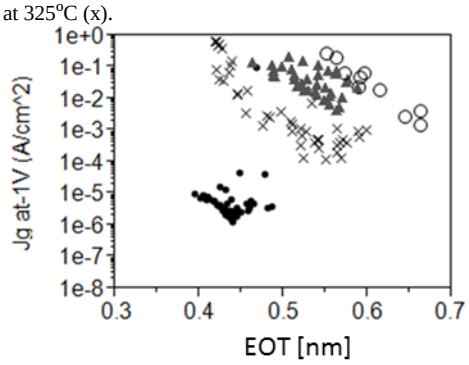

Fig.4b. EOT-J_g at -1V : Ru PVD (•), Ru EBECHRu at 325ºC (o), Ru Carish at 325ºC (▲), Ru EBECHRu with 5 min H_2 post - anneal at 325ºC (x).

A higher Sr content (e.g. 57 % Sr as compared to 54 %) led to a further increase of J_g. The decrease of the EOT and J_g during H_2 post-annealing further confirms that oxidation of the STO substrate is detrimental to the electrical characteristics of the films. Investigation of the $SrTiO_x$/Ru TE interface was needed to understand this behavior. For this purpose, SIMS depth profiling has been performed on Ru/$SrTiO_x$(57% Sr)/Si stacks with the results shown in Figure 5. Depth profiles of Sr species indicate a degree of Sr diffusion into the Ru layer for the ALD Ru processes, although no quantitative analysis could be performed in this case.

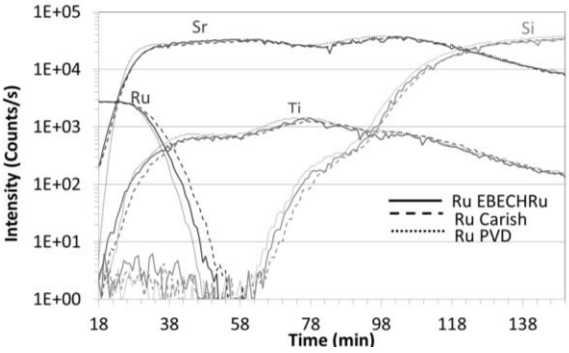

Fig.5. SIMS profiles of ^{99}Ru, ^{48}Ti and ^{88}Sr of the Ru/STO/Si stacks.

As ARXPS is a surface - sensitive technique, the elements present on the surface, like oxygen (O 1s), will give higher signal. Further, it can be observed that on average Ti is located deeper than Sr pointing as well to out-diffusion of Sr (Figure 6).

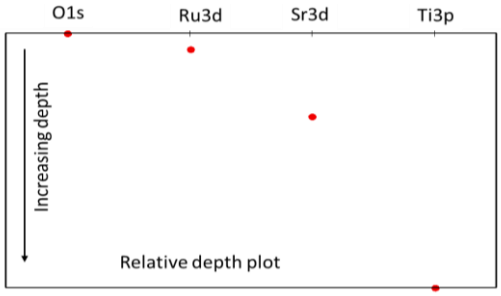

Fig.6. ARXPS derived relative depth plot of the constituent elements O1s, Ru3d, Sr3d and Ti3p for the Ru (Carish)/STO/Si stack from top surface to increased depth.

To quantify these observations MEIS analysis [8] has been carried out on 5nm Ru/7nm $SrTiO_x$(57% Sr)/Si stacks grown by the above ALD and PVD Ru processes. The energy spectrum obtained for the EBECHRu grown layer is shown in Figure 7a (signal). Scattering peaks are labeled.

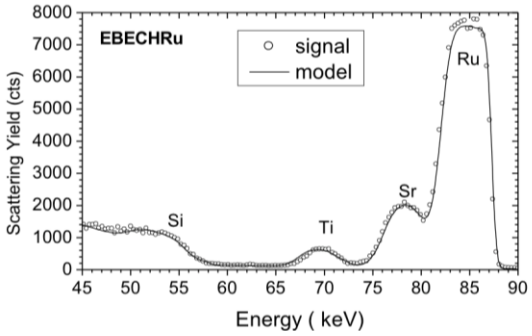

Fig. 7a. MEIS spectra of the EBECHRu grown 5nm Ru/7nm $SrTiO_x$/Si stack. (100 keV He ions and scattering angle 125°).

Detailed modeling using a MEIS spectrum simulation code [8] shows the occurrence of substantial inter-diffusion at the Ru/STO interface, albeit to different degrees for the 3 growth processes that results in the formation of a transition or interlayer. The stack layer structure derived from the best fit simulation (model) is shown in depth profile of Figure 7b.

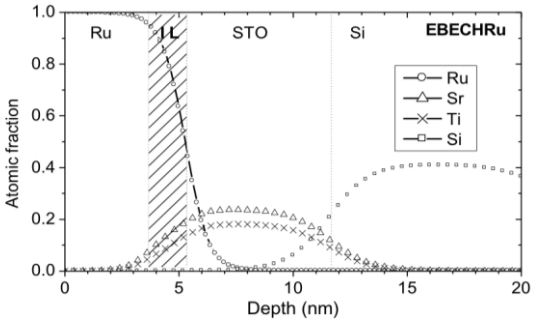

Fig.7b. MEIS profiles of Ru, Ti and Sr of the Ru/STO/Si stack.

Layer boundaries (marked at 50% height in Fig. 7b) reflect the nominal layer thicknesses well, as do the Sr/Ti ratios in the STO layer. More importantly, they confirm the formation of a interlayer (IL) typically 1.6-2.1 nm thick, at the Ru TE/$SrTiO_x$ interface the average composition of which can be quantified. This interlayer is formed for all three processes. However, comparative MEIS spectra clearly show that the PVD process leads to the sharpest Ru/STO interface followed by the ECBECHRu and Carish ones, respectively, in agreement with the SIMS profiles in Figure 5. The PVD process also results in the smallest amount of Ti incorporation into the interlayer. Average atomic compositions within the interlayers formed in the three processes, as obtained from MEIS depth profiles of the three stacks are given in Table 1, including their ratios.

Table 1. Average atomic percentages of Ru, Sr and Ti incorporated in the interlayer formed at STO/Ru TE interface and the relative ratio Ru/Sr and Sr/Ti for the three types of Ru TE (Ru PVD, Ru derived from the EBECHRu and Carish precursors, respectively by ALD).

Ru TE	PVD	EBECHRu	Carish
Ru [%]	83	76	79
Sr [%]	13	15	13
Ti [%]	4	9	8
Ru/Sr	6.4	5.1	6.1
Sr/Ti	3.3	1.7	1.6

It is clear that the PVD process apart from showing the sharpest Ru/STO interface, also leads to an incorporation of Ti into the interlayer that is significantly smaller than observed for the ALD processes, despite comparable Sr levels. The Ru/Sr ratios of the interlayers also show that relatively more Sr was incorporated for the case of the EBECHRu compared to the Carish precursor. Although no information could be gathered about the oxygen content of the interlayer, it is most likely that its presence during Ru ALD deposition plays a decisive role in formation of the interfacial oxide. The low dielectric constant (k) of the $SrRuTiO_x$ layer created at the Ru ALD/STO interface can explain the increase in the EOT and J_g. It is also probable that the larger increase in EOT for EBECHRu as compared to Carish precursor is due to a greater Sr incorporation in the former films. Another factor that may favor the interfacial reaction of Ru and STO is the thermal budget (namely deposition temperature and deposition time). Ru PVD is a room temperature process that requires about 8 min for the deposition of a 5 nm layer. However, a 5 nm Ru ALD deposition at 325 ºC requires ~ 47 minutes for the EBECHRu process and 19 minutes for the Carish one. Therefore, a larger increase in EOT for the same deposition temperature would be expected for the EBECHRu precursor. The role of temperature was shown when an alternative ALD Ru layer derived from EBECHRu was grown at 225ºC. In this case, the EOT increase was reduced by half the value obtained at 325 ºC. However, in this case the leakage current was considerably increased due to the poor quality Ru ALD that results at this temperature. Additionally, TiN deposited on top of the 225 ºC 5 nm ALD Ru could increase further the leakage current by scavenging oxygen from STO through the low density Ru ALD layer.

4. Conclusions

Sr and Ti out-diffusion from Sr rich $SrTiO_x$ into the Ru top electrode is shown to lead to a $SrRuTiO_x$ interlayer formation, which in turn was found to be responsible for the increase in EOT and J_g when employing Ru ALD aided by an O_2 co-reactant. A protective TiO_2 layer positively impacts the increase in EOT-J_g, but cannot provide a final solution due to the poor performance of the anatase TiO_2 in respect of leakage. Further work is required to identify a low temperature ALD Ru TE process that will minimize O_2 incorporation and reduce the interfacial SrTiOx/Ru reaction.

Acknowledgements

This work was carried out as part of imec's Industrial Affiliation Program funded by imec's Core Partners.

Tanaka Kikinzoku Group, Chemicals Materials Development Dep., Tsukuba Technical Center, Japan is acknowledged for providing the Ru Carish precursor.

References

[1]. M. Popovici, J. Swerts, A. Redolfi, B. Kaczer, M. Aoulaiche, I. Radu, S. Clima, J.-L. Everaert, S. Van Elshocht, M. Jurczak, Appl. Phys. Lett. 104 (2014) 082908, pp.1 – 5.

[2]. J. Swerts, M. Popovici, B. Kaczer, M. Aoulaiche, A. Redolfi, S. Clima, C. Caillat, W. C. Wang, V. V. Afanas'ev, N. Jourdan, C. Olk, H. Hody, S. Van Elshocht, M. Jurczak, IEEE Electron Device Lett. 35 (2014), pp. 753-755.

[3]. M. Popovici, S. Van Elshocht, N. Menou, J. Swerts, D. Pierreux, A. Delabie, B. Brijs, T. Conard, K. Opsomer, J. W. Maes, D. J. Wouters, J. A. Kittl, J. Electrochem. Soc. 157 (2010), pp. G1-G6.

[4]. B. Kaczer, S. Clima, K. Tomida, B. Govoreanu, M. Popovici, M.-S. Kim, J. Swerts, A. Belmonte, W.-C. Wang, V. V. Afanas'ev, A. S. Verhulst, G. Pourtois, G. Groeseneken, M. Jurczak, J. Vac. Sci. Technol. B 31 (2013) 01A105, pp. 1-5

[5]. A. Delabie, R. L. Puurunen, B. Brijs, M. Caymax, T. Conard, B. Onsia, O. Richard, W. Vandervorst, C. Zhao, M. M. Viitanen, H. H. Brongersma, M. de Ridder, L. V. Goncharova, E. Garfunkel, T. Gustafsson, W. Tsai, M. M. Heyns, M. Meuris, J. Appl. Phys. 97 (2005) 064104, pp. 1-10.

[6]. M. Popovici, J. Swerts, K. Tomida, D. Radisic, M.-S. Kim, B. Kaczer, O. Richard, H. Bender, A. Delabie, A. Moussa, C. Vrancken, K. Opsomer, A. Franquet, M. A. Pawlak, M. Schaekers, L. Altimime, S. Van Elshocht, J.A. Kittl, Phys. Status Solidi RRL 5 (2011), pp. 19–21.

[7]. ITRS Reports, Section Front End Processes (FEP), FEP_2012 Tables, 2012 edition, online available at www.itrs.net (2012).

[8]. J.A. van den Berg, M.A. Reading, P. Bailey, T.Q.C. Noakes, C. Adelmann, M. Popovici, H. Tielens, T. Conard, S. de Gendt, S. van Elshocht, Appl. Surf. Sci. 281 (2013), pp. 8-16.